

Quantum Science and Technology



PAPER

Temporal correlations of spectrally narrowband photon pair sources

OPEN ACCESS

RECEIVED

23 December 2016

REVISED

17 March 2017

ACCEPTED FOR PUBLICATION

5 April 2017

PUBLISHED

8 May 2017

Original content from this work may be used under the terms of the [Creative Commons Attribution 3.0 licence](#).

Any further distribution of this work must maintain attribution to the author(s) and the title of the work, journal citation and DOI.



Kai-Hong Luo¹, Harald Herrmann and Christine Silberhorn

Integrated Quantum Optics, Applied Physics, University of Paderborn, Warburger Str. 100, D-33098, Paderborn, Germany

¹ Author to whom any correspondence should be addressed.

E-mail: khluo@mail.uni-paderborn.de

Keywords: integrated quantum optics, photon counting and statistics, single-photon detection

Abstract

We report on theoretical and experimental investigations of time-resolved cross- and auto-correlation measurements of spectrally narrowband photon pairs generated in sources based on parametric down conversion in resonant waveguide structures. We show that time-resolved measurements provide detailed and useful information about the spectral and modal structure of the bi-photon state. The shape of the cross-correlation function is asymmetric with exponential decays determined by the lifetimes of the signal and idler photons in the cavity. The time-resolved auto-correlation has Lorentzian shape. The measured $g^{(2)}(0)$ value convoluted with the detector windows and mode beating can be used to characterise the spectral longitudinal mode behaviour. The temporal width of the auto-correlation function is more than two times longer than the cross-correlation time. This reveals that the spectral bandwidth of the single-photon component is much broader than the spectral width of the two-photon component.

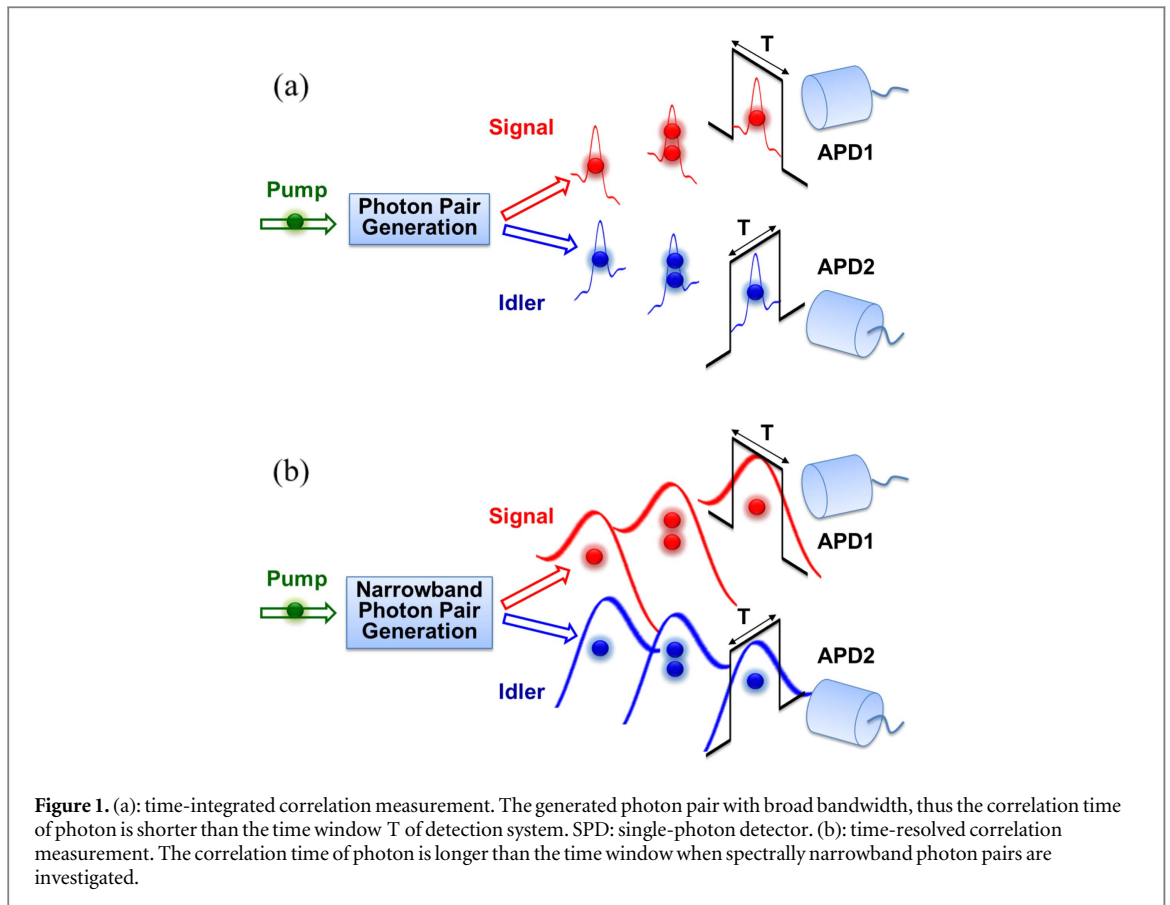
Single-photon detection and, in particular, coincidence measurements [1, 2] based on second (and higher) order spatial and temporal correlations are essential for almost all kinds of quantum optic experiments [3–8]. In general, encoding, manipulating and shaping photons in quantum communication, quantum cryptography and quantum networking, all of which rely on how single photons are detected and counted. However, due to the limited time resolution of current single-photon detection systems, the detection process is often not fast enough to reveal all photon properties.

Over the last several decades single-photon detection has made tremendous progress. Based on different technologies beginning with traditional photomultipliers via solid-state avalanche photodiodes to superconducting nanowire or transition edge detectors a variety of single-photon detectors (SPD) have been developed and optimised. However, due to the current limitations of the technology, even the fastest SPDs based on superconducting nanowires (~tens of ps) are still several orders of magnitude slower than the temporal width of photons (~ps or even less) from typical parametric down conversion (PDC) or four-wave mixing sources, which are mostly used in quantum optics experiments. As a result, the exact timing of every photon cannot be resolved with such time-integrated detectors.

A way to reveal more details of the timing is to use a PDC source that generates narrowband photon pairs (NPP), i.e. a source that produces photons with a temporal width exceeding the time window of the SPD. It has already been shown that temporal coincidence measurements between narrowband photons can be used to determine the spectral bandwidth of these photons, even for cases where traditional spectrometry cannot resolve the linewidth [9–16].

The objective of this work is to study which information of the source can be determined from measurements of correlation functions with a resolution, which is better than the temporal width of the photons. It is known from photon-number resolved detection [17–19] that the statistics of multiple photon pairs [20] effects on the heralding rates, single-photon fidelities [21] and other quantum effects. Our goal is to investigate whether we can retrieve from time-resolved correlation measurements further details of the sources.

To do such investigations, we need narrowband PDC sources. In principle, two ultra-narrow filters can be used to filter down the spectral widths of standard photon pair sources. However, this is not easy to operate in

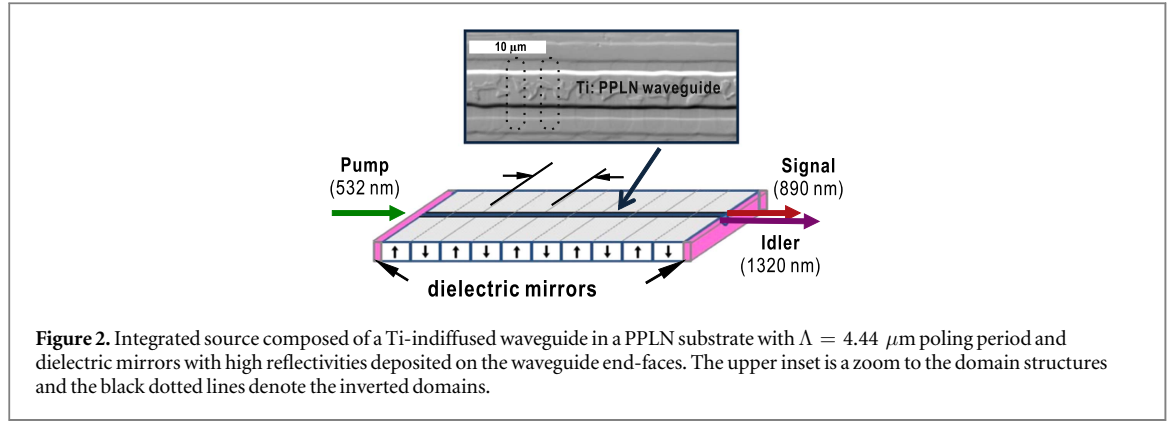


practical terms because to systematically investigate the temporal behaviour of single and multiple photon pairs generation, the practical implementation requires several NPP sources with high brightness, excellent stability, compact design and easy operation.

We investigated two different miniaturised photon pair sources based on doubly resonant waveguides exhibiting one or several longitudinal modes [22]. These investigations enabled us to resolve temporal structures of the cross-correlation between signal and idler and the auto-correlation of two-photon components, which are usually covered by the detector jitter when broadband photon pairs are investigated. Thus, the more information of cross and auto-correlation functions, such as temporal shape, correlation time and mode behaviour can be revealed.

Figure 1 illustrates the basic scheme of our measurements. Figure 1(a) shows the standard time-integrated correlation measurement. The spectrally broad photon pairs lead to a temporarily narrow correlation, which cannot be resolved due to jitter in the SPDs which limits the resolution of the SPD to an effective detector window T . However, if the photon pair is spectrally narrowband, the temporal structure of the correlation is broader than this detection window (as sketched in figure 1(b)); thus, temporal structures of the correlation functions can be investigated.

A widespread method to generate NPP is cavity-enhanced PDC. In such a nonlinear process, a single pump photon splits into two photons (signal and idler) inside a cavity, obeying energy conservation, phase matching and resonance conditions. For our experiments, we used miniaturised integrated photon pair sources that are based on doubly resonant waveguides exploiting type II PDC phase matching in a Ti-indiffused periodically poled LiNbO₃ (PPLN) waveguide. A schematic sketch of the integrated source is shown in figure 2. The end-faces of the waveguide are directly coated with high-reflective dielectric mirrors to form the cavity. In the dispersive waveguide, cavity resonances occur at distinct frequencies separated by the free spectral range (FSR) of the resonator. These resonances form Lorentzian frequency combs spaced with respective FSRs in the signal and idler wavelength range. Because of different FSRs in the resonant waveguide due to the different dispersions at the signal and idler wavelengths and polarisations, the resonances of signal and idler only overlap at certain frequencies, so called ‘cluster’. As maximum enhancement is only obtained if both signal and idler are resonant simultaneously, PDC is generated only in such cluster regions of the spectrum.



Including multiple photon pairs generation up to the second-order, the photon pair states generated within such a resonator can be expressed by

$$|\Psi\rangle_{\text{RPDC}} \propto \int d\omega_s d\omega_i f_R(\omega_s, \omega_i) \hat{a}_s^\dagger(\omega_s) \hat{a}_i^\dagger(\omega_i) |0\rangle + \int d\omega_s d\omega'_s d\omega_i d\omega'_i f_R(\omega_s, \omega_i) f_R(\omega'_s, \omega'_i) \times \hat{a}_s^\dagger(\omega_s) \hat{a}_s^\dagger(\omega'_s) \hat{a}_i^\dagger(\omega_i) \hat{a}_i^\dagger(\omega'_i) |0\rangle, \quad (1)$$

where $f_R(\omega_s, \omega_i)$ is the cavity-modified joint spectral function (JSF) determined by pump spectral distributed function, phase-matching function and field distributions inside the cavity. When signal and idler are both resonant simultaneously in a dispersive cavity, we can approximate the individual cavity resonance by a Lorentzian function $(\gamma_{s,i} + i\omega_{s,i})^{-1}$, where $\gamma_{s,i}$ describes the damping constants of cavity at signal and idler frequency, respectively. If there is only one pair of signal and idler cavity modes with narrowband range $\delta\omega$ generated (or filtered) in the centre of phase matching, we obtain a complex JSF:

$$f_R(\delta\omega) \approx \frac{\gamma_s \gamma_i}{\gamma_s + i\delta\omega \gamma_i - i\delta\omega}. \quad (2)$$

The temporal signal-idler cross-correlation function $g_{si}^{(1,1)}(\tau)$ is measured as the coincidence distribution of time differences between the signal and idler photons $\tau = t_s - t_i$. Using the inverse Fourier transform of the JSF, the signal-idler correlation can be simplified to

$$g_{si}^{(1,1)}(\tau) = \langle \hat{a}_s^\dagger(t) \hat{a}_i^\dagger(t + \tau) \hat{a}_i(t + \tau) \hat{a}_s(t) \rangle \propto u(\tau) e^{-2\gamma_s \tau} + u(-\tau) e^{2\gamma_i \tau}, \quad (3)$$

where $u(\tau)$ is the step function. In general, i.e. if $\gamma_s \neq \gamma_i$, the correlation function is not longer symmetric. For $\tau < 0$ the correlation function raises exponentially with a time constant $\tau_s = (2\gamma_s)^{-1}$, whereas the exponential decay for $\tau > 0$ drops with $\tau_i = (2\gamma_i)^{-1}$. Thus, the width of the correlation function is determined by the lifetimes of the signal and idler photons in the cavity. For the following, we define the signal-idler correlation time to be $\tau_c = 2(\tau_s + \tau_i)/e$.

The normalised second-order auto-correlation function is given by $g^{(2)}(\tau)$:

$$g^{(2)}(\tau) = 1 + \left| \frac{\langle \hat{a}^\dagger(t) \hat{a}(t + \tau) \rangle}{\langle \hat{a}^\dagger(t) \hat{a}(t) \rangle} \right|^2 = 1 + |g^{(1)}(\tau)|^2. \quad (4)$$

Similar to the derivation of the signal-idler correlation function, we consider a signal cavity mode with a Lorentzian spectral distribution and use the inverse Fourier transform of its intensity spectrum. Then, equation (4) can be approximately simplified to

$$g_{ss}^{(2)}(\tau) \approx 1 + \left(1 + \left[\frac{1}{2}(\gamma_s + \gamma_i)\tau \right]^2 \right)^{-1}. \quad (5)$$

Obviously, this auto-correlation function is symmetric no matter which kind of PDC process it produced. This is different compared to cross-correlation function $g_{si}^{(1,1)}(\tau)$ with its asymmetrical exponential decays out from cavity. In principle, this asymmetrical behaviour is from the cavity-modified JSF $f_R(\omega_s, \omega_i)$, which has the chirped phase from signal and idler resonance. The shape of the auto-correlation function is of a type of a Cauchy-Lorentz distribution. The auto-correlation time of signal photon T_{au}^{ss} is approximately given by

$$T_{au}^{ss} \approx \frac{4}{\gamma_s + \gamma_i}. \quad (6)$$

Together with the signal-idler correlation time τ_c , we have

$$T_{au}^{ss} \approx \frac{2}{\ln 2} \tau_c, \quad (7)$$

which exceeds the cross-correlation time by a factor around 2.8.

Concerning the multi-mode cases, we assume that several pairs of signal ω_{sn} and idler modes ω_{in} are generated from the resonant PDC source. The time-dependent signal-idler correlation function can be generalised to

$$g_{si,multi}^{(1,1)}(\tau) \propto u(\tau) e^{-2\gamma_s \tau} \left| \sum_n s_n e^{-i\omega_{sn}\tau} \right|^2 + u(-\tau) e^{2\gamma_i \tau} \left| \sum_n s_n e^{i\omega_{in}\tau} \right|^2. \quad (8)$$

The absolute square interference term tells us that for the multi-mode case a beating under the exponentially decaying envelope occurs. In the same way, the multi-mode auto-correlation function is given as

$$g_{multi}^{(2)}(\tau) = 1 + \frac{1}{N} |g_0(\tau)|^2 + \frac{1}{N^2} \sum_{n=1}^{N-1} 2(N-n) \cos[n\Delta_F \tau] |g_0(\tau)|^2, \quad (9)$$

where $g_0(\tau)$ is the inverse Fourier transform of signal (or idler) intensity, Δ_F is the angular FSR and N is the number of modes. For a perfect time resolution, we always get $g_{multi}^{(2)}(0) = 2$. However, using real detectors with their finite temporal resolution, the measured $g_m^{(2)}(0)$ is always a convolution of the real $g_{multi}^{(2)}(\tau)$ with the detection window. Thus, the fast beating of $g_{multi}^{(2)}(\tau)$ under the exponentially decaying envelope lowers the measured $g_m^{(2)}(0)$. In a realistic scenario, the detection window is in the range of 0.5 ns and Δ_F is in the order of tens to hundreds of GHz. Thus, the time window of the detection system covers several beating periods, hence the measured $g_m^{(2)}(0)$ will be

$$g_m^{(2)}(0) \approx 1 + \frac{1}{N}. \quad (10)$$

Consequently, the number of cavity modes N can be directly estimated from the auto-correlation value. Please note that this conclusion is similar with pulsed time-integrated correlation in [23], although finite time-resolved correlation function is different with time-integrated one. Figure 3 provides the calculated coincidences between signal and idler photon generated from the double cavities. The simulated and convoluted auto-correlation results for signal photons from two resonant waveguides are theoretically predicted as well.

To study experimentally the correlation between photon pairs, two different resonant PDC waveguide sources given in table 1 were investigated. They are composed of a 12.3 mm (first source) and 14.5 mm (second source) long Ti-indiffused waveguide which is periodically poled with a poling period of 4.44 μm to provide type II phase matching for a PDC process pumped at 532 nm to generate nondegenerate photon pairs around 890 nm (signal) and 1320 nm (idler). Both sources have a front mirror with a high reflectivity ($R_{f1} \approx R_{f2} \approx 99\%$) for signal and idler wavelengths. The rear mirror of the first source has also a high reflectivity ($R_{r1} \approx 99\%$), whereas the reflectivity of the rear mirror of the second source is only $R_{r2} \approx 90\%$. The cavity finesse of the first source is $\mathcal{F}_{s1} \sim 100$ and $\mathcal{F}_{i1} \sim 80$ for the signal and idler wavelengths, respectively, while the second has a lower finesse of $\mathcal{F}_{s2} \sim 22$ and $\mathcal{F}_{i2} \sim 25$. The experimental characterisation of such resonant waveguide device has already been discussed in detail in [22]. Here we only focus on revealing the correlation information from different samples which is not covered by the time resolution of detector system.

The PDC spectra of both sources consist of three clusters with a spectral separation of about 90 GHz and 75 GHz, individually. A volume Bragg grating is inserted into the signal beam to act as bandpass filter to select a single cluster. The modal structure within the selected cluster was investigated using a confocal scanning Fabry–Perot resonator with a free spectral range of 15 GHz (figures 4 (a) and (b)). These measurements revealed the modal structure of our sources: the first one operated only on a single longitudinal mode, whereas in the second one with the lower finesse three longitudinal modes with different strength could be observed. Please note that the periodical peaks are due to the scan of FP through three FSRs of FP etalon. With these measurements, the spectral bandwidth of the longitudinal modes could not be determined because the Fabry–Perot resonator has only a resolution of about 700 MHz, which is much larger than the expected bandwidth of the PDC modes.

Cross- and auto-correlation measurements were performed using these two sources. In figures 4 (c) and (d), signal-idler cross-correlation coincidence results are shown. The presence of the cavity implies that the shape of the coincidence curve should be determined by exponential functions. This is in good accordance with the theoretical prediction, as shown in equation (3). The slight asymmetry reflects the different finesesses of signal and idler resulting in slightly different leakage times out of the resonator. The different slopes of decay predict the different decay times. The cross-correlation times are around 4.8 ns and 2.1 ns, respectively. According to $\tau_c = 1/\pi\Delta\nu$, where $\Delta\nu$ is the bandwidth of the down-converted photons, a spectral bandwidth of about 60 MHz and 150 MHz can be deduced.

Figures 4(e) and (f) provide the convoluted auto-correlation results for signal photons. For single or multiple cavity modes, for ideal detection, the expected $g^{(2)}(0)$ value is close to 2. When more cavity modes are involved,

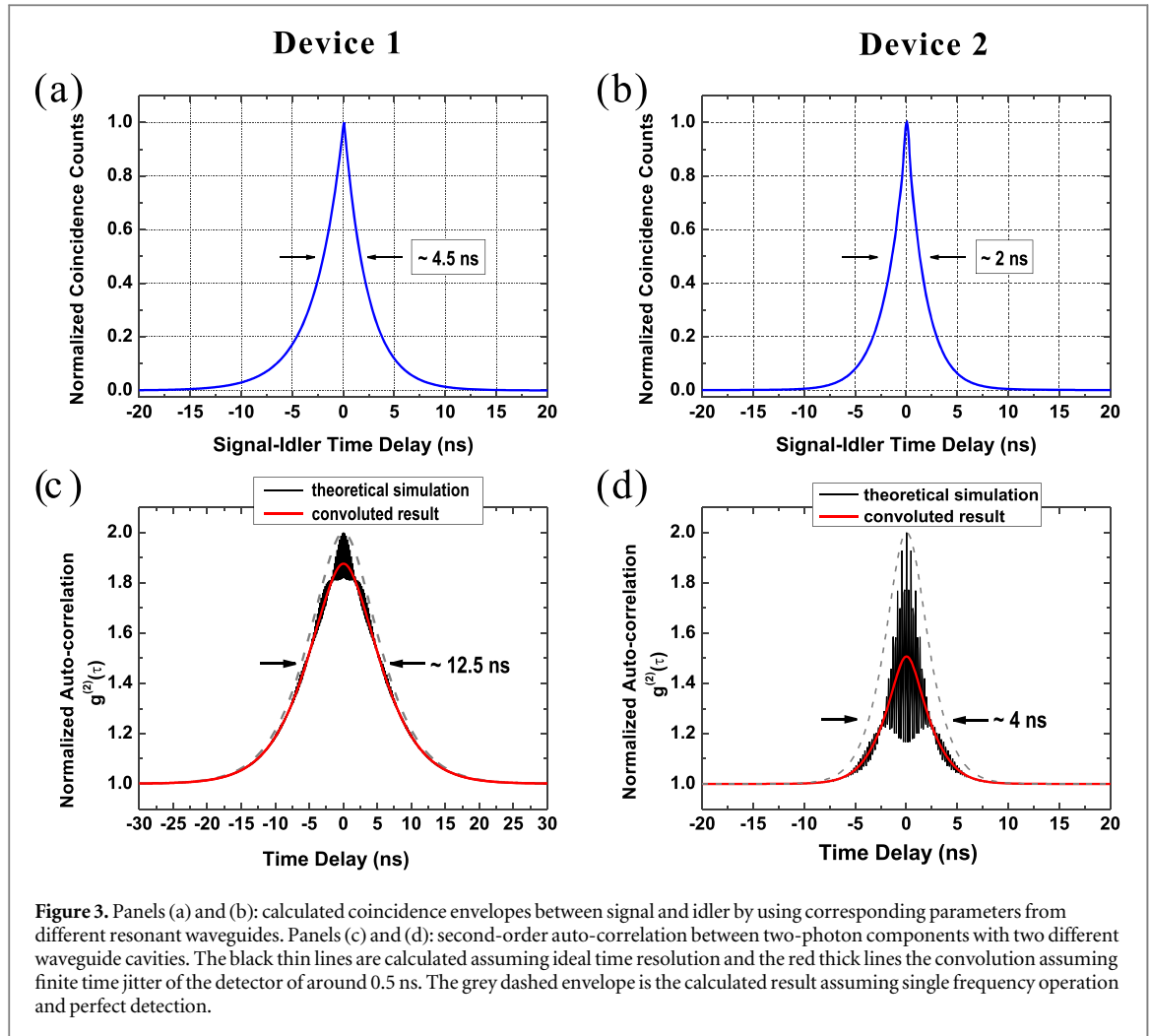


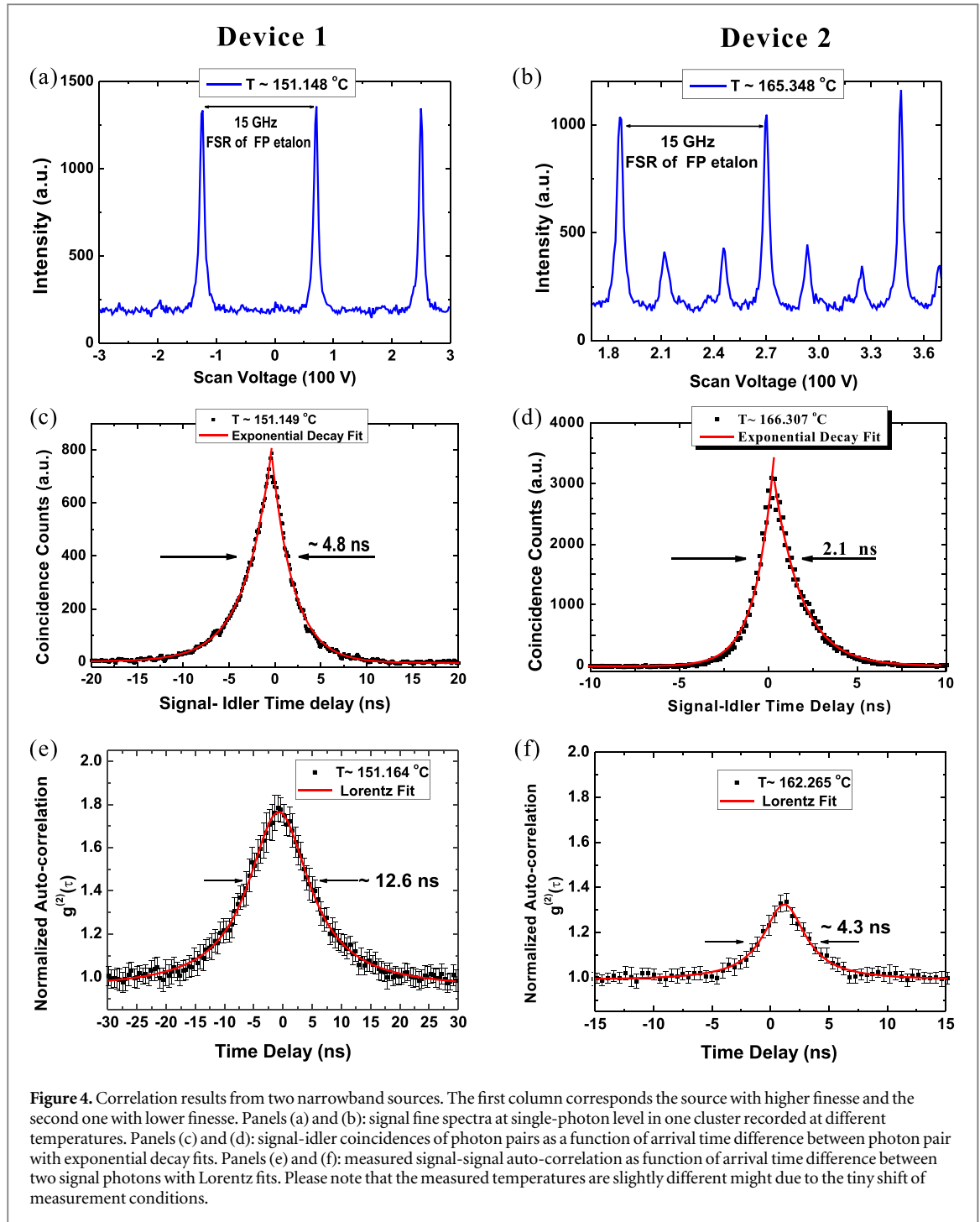
Figure 3. Panels (a) and (b): calculated coincidence envelopes between signal and idler by using corresponding parameters from different resonant waveguides. Panels (c) and (d): second-order auto-correlation between two-photon components with two different waveguide cavities. The black thin lines are calculated assuming ideal time resolution and the red thick lines the convolution assuming finite time jitter of the detector of around 0.5 ns. The grey dashed envelope is the calculated result assuming single frequency operation and perfect detection.

Table 1. Device properties of two different resonant waveguides.

Resonant waveguide	Device 1	Device 2
Length	$L_1 \approx 12.3$ mm	$L_2 \approx 14.5$ mm
Front reflectivity	$R_{f1} \approx 99\%$	$R_{f2} \approx 99\%$
Rear reflectivity	$R_{r1} \approx 99\%$	$R_{r2} \approx 90\%$
Signal finesse	$\mathcal{F}_{s1} \sim 100$	$\mathcal{F}_{s2} \sim 22$
Idler finesse	$\mathcal{F}_{i1} \sim 80$	$\mathcal{F}_{i2} \sim 25$
Cluster separation	90 GHz	75 GHz

the measured value is a convolution between mode beating and detector resolution. It causes the low measured $g_m^{(2)}(0)$ value in the finite detector window. From the measured values $g_{m1}^{(2)}(0) \approx 1.85$ and $g_{m2}^{(2)}(0) \approx 1.35$, the effective cavity mode number of $N_1 \approx 1.2$ and $N_2 \approx 2.8$, respectively, can be estimated. This is in reasonably good qualitative agreement with the theory and the measured spectra shown in figures 4(a) and (b). The signal auto-correlation time ($T_{au1}^{ss} \sim 12.5$ ns) is about 2.8 times broader than the signal-idler correlation time ($\tau_{c1} \sim 4.8$ ns), which is matched well a theoretical analysis using equation (7). A Lorentzian fit to experimental curve also coincides with our theory. For the lower finesse sample, T_{au2}^{ss} (around 4 ns) is only two times longer than τ_{c2} (~ 2 ns). The reason why this measured value deviates more from the theoretically predicted than corresponding results for the high finesse source is that the correlation time is close to the time resolution of the detection system (~ 0.5 ns). Thus, this measurement is partially but not completely time-resolved. This clearly reveals that interpreting such measurements requires a careful analysis of the timing resolution of the measurement system.

The results can also be understood by using another but equivalent interpretation looking at the signal or idler multi-photon contributions. These arise from the second term in equation (1). Whereas the cross-correlation coincidences mostly occur from single-photon pair generation events, i.e. the first term in equation (1), the auto-correlation is solely due to the multi-photon contributions. Thus, there are different parts



of the photon pair states which are probed by the cross-correlation and the auto-correlation measurements. The auto-correlation time T_{au} is the correlation time between two (signal or idler) photon components, while the cross-correlation time τ_c is the correlation time between signal and idler photons. From the experimental investigations and also from our theoretical considerations, we showed that the auto-correlation time T_{au} is larger than correlation time τ_c . Correspondingly, the two-photon components have a narrower frequency bandwidth (related to the product $f_R(\omega_s, \omega_i)f_R(\omega'_s, \omega'_i)$) than then the one-pair component (related to $f_R(\omega_s, \omega_i)$) in the spectral domain. Intuitively, there is a higher probability to generate multiple photon pairs in the centre of phase-matching condition. Therefore, it is easily understandable that single-photon pairs and multiple photon pairs have different spectral and temporal properties.

In summary, we have theoretically and experimentally investigated correlation measurements and the relation to the temporal resolution of the detection system. For this purpose we investigated different narrowband photon pair sources based on PDC in doubly resonant PPLN waveguides. We showed that cross- and auto-correlation functions have different temporal shapes: the cross-correlation has asymmetric exponential decays whereas the auto-correlation is of Lorentzian shape. The temporal width of the auto-

correlation function is longer than the cross-correlation time. Thus, we could conclude that the two-photon pair part of the PDC state is spectrally narrower than the single pair contribution. Additionally, we analysed how the measured $g^{(2)}(0)$ is influenced by the timing jitter of the detection system, e.g. we could relate the measured $g^{(2)}(0)$ value with the number of longitudinal modes from our sources.

From our investigations, we can conclude that a profound understanding of temporal and spectral correlations is of key importance. A detailed knowledge of the physics behind time-resolved measurements provides essential insight for analysing source properties. What we have learned from the time-resolved detection can generally be used to other narrowband sources as well, but the correlation shape is associated with the generation mechanism of narrowband sources. Thus, such time-resolved measurements are useful tool in particular for optimised engineering of all kinds of narrowband photon pair sources.

Acknowledgements

This work was supported by the Deutsche Forschungsgemeinschaft via SFB TRR 142 and via the Gottfried Wilhelm Leibniz-Preis.

References

- [1] Hanbury Brown R and Twiss R Q 1956 *Nature* **177** 27
- [2] Glauber R J 1963 *Phys. Rev.* **131** 2766
- [3] Gisin N, Ribordy G, Tittel W and Zbinden H 2002 *Rev. Mod. Phys.* **74** 145
- [4] Lvovsky A I, Sanders B C and Tittel W 2009 *Nat. Photon.* **3** 706
- [5] Zhang H et al 2011 *Nat. Photon.* **5** 628
- [6] Tanzilli S et al 2012 *Laser & Photonics Reviews* **6** 115
- [7] Spring J B et al 2013 *Science* **339** 798
- [8] Morin O, Fabre C and Laurat J 2013 *Phys. Rev. Lett.* **111** 213602
- [9] Ou Z Y and Lu Y J 1999 *Phys. Rev. Lett.* **83** 2556
- [10] Kuklewicz C E, Wong F N C and Shapiro J H 2006 *Phys. Rev. Lett.* **97** 223601
- [11] Scholz M, Koch L and Benson O 2009 *Phys. Rev. Lett.* **102** 063603
- [12] Wolgramm F, de Icaza Astiz Y A, Beduini F A, Cerè A and Mitchell M W 2011 *Phys. Rev. Lett.* **106** 053602
- [13] Chuu C-S, Yin G Y and Harris S E 2012 *Appl. Phys. Lett.* **101** 051108
- [14] Förtsch M et al 2013 *Nat. Commun.* **4** 1818
- [14] Förtsch M et al 2015 *Phys. Rev. A* **91** 023812
- [15] Fekete J, Rieländer D, Cristiani M and de Riedmatten H 2013 *Phys. Rev. Lett.* **110** 220502
- [16] Yan H et al 2011 *Phys. Rev. Lett.* **106** 033601
- [17] Achilles D et al 2004 *J. Mod. Opt.* **51** 1499
- [18] Rosenberg D, Lita A E, Miller A J and Nam S W 2005 *Phys. Rev. A* **71** 061803
- [19] Kardynal B E, Yuan Z and Shields A J 2008 *Nat. Photonics* **2** 425
- [20] Wasilewski W, Radzewicz C, Frankowski R and Banaszek K 2008 *Phys. Rev. A* **78** 033831
- [21] U'Ren A B, Silberhorn C, Banaszek K and Walmsley I A 2004 *Phys. Rev. Lett.* **93** 093601
- [22] Luo K-H et al 2015 *New J. Phys.* **17** 073039
- [23] Christ A, Laiho K, Eckstein A, Cassemiro K N and Silberhorn C 2011 *New J. Phys.* **13** 033027